Colloid stability 2

Potential energy curves

The total energy of interaction between the particles in a lyophobic sol is obtained by summation of the electric double layer and van der Waals energies, as illustrated in Figure 8.2.

The general character of the resulting potential energy-distance curve can be deduced from the properties of the two components.

For the interaction between particles of the same material, the double-layer repulsion energy (equation (5)) is an approximately exponential function of the distance between the particles with a range of the order of the thickness of the double layer ($1/\kappa$), and the van der Waals attraction energy (equation (10)) decreases as an inverse power of the distance between the particles. Consequently, van der Waals attraction will predominate at small* and at large interparticle distances. At intermediate distances double-layer repulsion may predominate, depending on the actual values of the two forces. Figure 8.2 shows the two general types of potential energy curve which are possible. The total potential energy curve *V(1)* shows a repulsive energy maximum, whereas in curve *V(2)* the double-layer repulsion does not predominate over van der Waals attraction at any interparticle distance.

**(Repulsion due to overlapping of electron clouds (Born repulsion) predominates at very small distances when the particles come into contact, and so there is a deep minimum in the potential energy curve which is not shown in Figures 8.2-8.4.)*

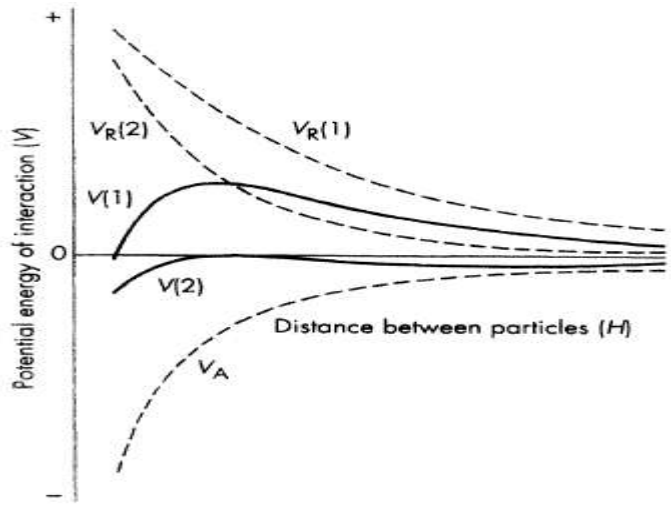

Figure 8.2 Total interaction energy curves, V(l) and V(2), obtained by the summation of an attraction curve, *VA*, with different repulsion curves, VR(1) and VR(2)

If the potential energy maximum is large compared with the thermal energy *kT* of the particles, the system should be stable; otherwise, the system should coagulate. The height of this energy barrier to coagulation depends upon the magnitude of ψ_d (and ξ) and upon the range of the repulsive forces (i.e. upon $1/\kappa$), as shown in Figures 8.3 and 8.4.

Figures 8.3 and 8.4 shows the potential energy maxima at inter-particle separations of a few nanometers, Surface roughness of at least up to this magnitude is, therefore, unlikely to invalidate these potential energy calculations.

Secondary minima

Another characteristic feature of these potential energy curves is the presence of a secondary minimum at relatively large interparticle distances. If this minimum is moderately deep compared with *kT*, it should give rise to a loose, easily reversible flocculation. For small particles (a < *c.* 10~8 m) the secondary minimum is never deep enough for this to happen in those cases where the potential energy maximum is high enough to prevent coagulation into the primary minimum. If the

particles are larger, flocculation in the secondary minimum may cause observable effects.

Several colloidal systems containing anisodimensional particles, such as iron oxide and tobacco mosaic virus sols, show reversible separation into two phases when the sol is sufficiently concentrated and the electrolyte concentration is too low for coagulation in the primary minimum. One of the phases is a dilute isotropic sol, the other a more concentrated birefringent sol. The particles in the birefringent phase are regularly aligned as parallel rods or plates 10-100 nm apart (the distance depending on the pH and ionic strength of the sol)

Secondary minimum flocculation is considered to play an important role in the stability of certain emulsions and foams.

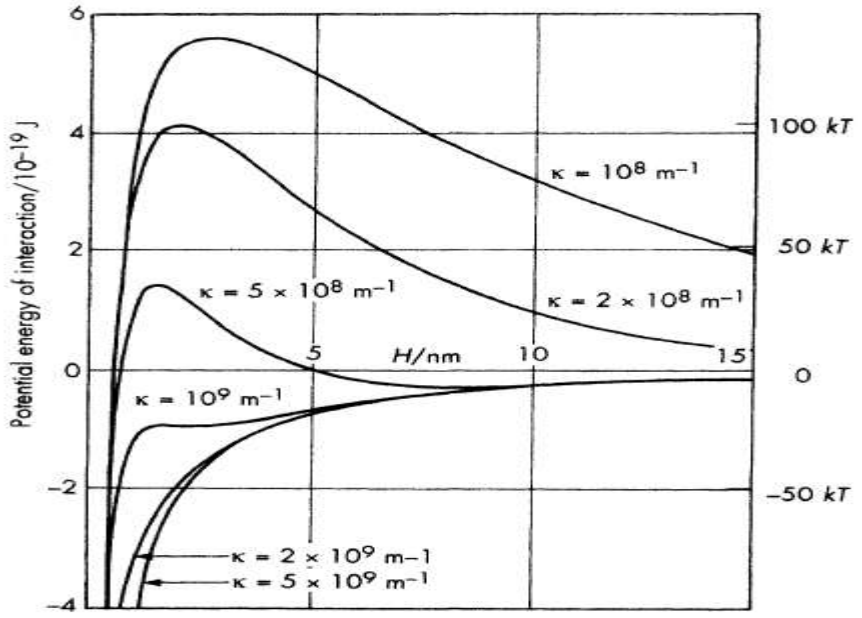

Figure 8.3 The influence of electrolyte concentration, κ, on the total potential energy of interaction of two spherical particles: $a = 10^{-7}$ m; $T = 298$ K; $z = 1$; $A_{11} = 2 \times 10^{-19}$ J; $A_{33} = 0.4 \times 10^{-19}$ J; $\epsilon/\epsilon_0 = 78.5$; $\psi_d = 50$ mV $\approx 2kT/e$. V_R and V_A calculated using equations (8.7), (8.9) and (8.13)

Measurement of particle interactions

Owing to their fundamental interest and their practical importance in issues such as colloid stability, much experimental effort has been devoted to the measurement of electric double layer and van der Waals interactions between macroscopic objects at close separations.

Such measurements involve balancing the force(s) to be measured with an externally applied force.

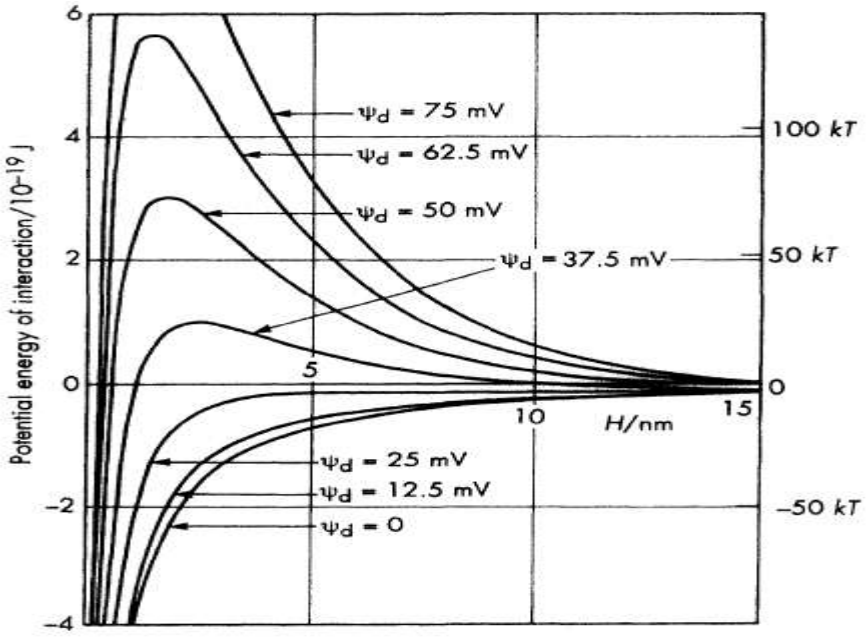

Figure 8.4 The influence of Stern potential, ψ_d, on the total potential energy of interaction of two spherical particles: $a = 10^{-7}$ m; $T = 298$ K; $z = 1$; $A_{11} = 2 \times 10^{-19}$ J; $A_{33} = 0.4 \times 10^{-19}$ J; $\epsilon/\epsilon_0 = 78.5$; $\kappa = 3 \times 10^8$ m^{-1}. V_R and V_A calculated using equations (8.7), (8.9) and (8.13)

Electric double layer interactions

Ottewill and co-workers have used a compression method to measure the double-layer repulsion between the plate-like particles of sodium montmorillonite. This is a particularly suitable system for such studies, since the particles are sufficiently thin (1 nm) for van der Waals forces to be unimportant and surface roughness is not a problem. The dispersion was confined between a semipermeable filter and an impermeable elastic membrane and an external pressure was applied via a hydraulic fluid so that the volume concentration of particles and, hence, the distance of separation between the particles could be measured as a function of applied pressure.

In another method, Roberts and Tabor measured the electric double layer repulsion between a transparent rubber sphere and a plane glass surface

separated by surfactant solution. As the surfaces were brought together, the double-layer interaction caused a distortion of the rubber surface which was monitored interferometrically.

The results of these measurements are in reasonable agreement with predictions based on electric double layer theory, especially at separations greater than $1/\kappa$.

Van der Waals interactions

Attractive forces between macroscopic objects have been measured directly by a number of investigators. In the first experiment of this kind, Deryagin and Abricossova used a sensitive electronic feed-back balance to measure the attraction for a Plano-convex polished quartz system from which all residual electric charge had been removed. Relatively large separations were involved and the measured attractive forces were consistent with those predicted by theory, provided that retardation was allowed for. Recently, measurements in the non-retarded range have been made, the most notable being those of Tabor and co-workers, on the attraction between cleaved layers of mica stuck to two crossed cylinders. In addition to providing successful tests of the distance dependence of the van der Waals attraction, the effects of adsorbed monolayers have also been studied, again giving reasonable agreement with theoretical predictions.

Structural interactions

Both Hamaker and Lifschitz theories of van der Waals interaction between particles are continuum theories in which the dispersion medium is considered to have uniform properties. At short distances (i.e. up to a few molecular diameters) the discrete molecular nature of the dispersion medium cannot be ignored. In the vicinity of a solid surface, the constraining effect of the solid and the attractive forces between the solid and the molecules of the dispersion medium will cause these molecules to

pack, as depicted schematically in Figure 8.5. Moving away from the solid surface, the molecular density will show a damped oscillation about the bulk value. In the presence of a nearby second solid surface, this effect will be even more pronounced.

The van der Waals interaction will, consequently, differ from that expected for a continuous dispersion medium. This effect will not be significant at liquid-liquid interfaces where the surface molecules can overlap, and its significance will be difficult to estimate for a rough solid surface.

Achvilli and co-workers have measured directly the forces between molecularly smooth cleaved mica surfaces separated by organic liquids and have observed a corresponding periodicity of force with separation. The extent to which these short-range interactions (solvation or structural forces) may influence colloid stability and other related phenomena is not entirely clear.

Particle adhesion

The adhesion of colloidal particles to solid substrates is of fundamental and technological importance (e.g. pneumatic transport of powders, printing, filtration, detergency, air pollution). In general, the principles developed in this chapter for particle-particle interactions apply also to particle-solid substrate interactions. Many indirect methods involving centrifugation, vibration, etc., have been developed to measure the force required to detach particles from a solid surface

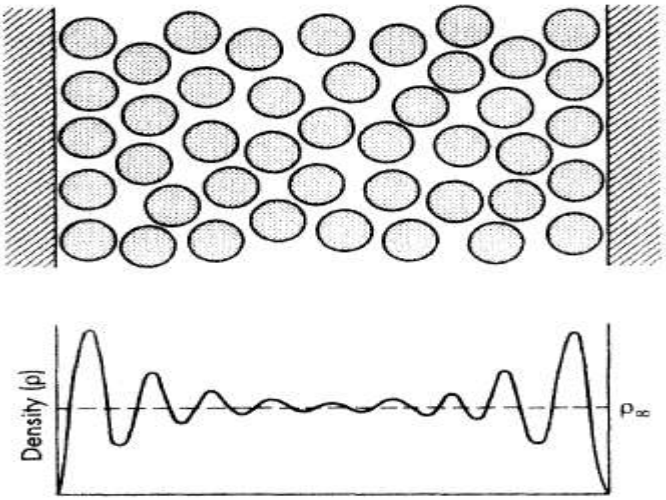

Figure 8.5 Distribution and density of dispersion medium molecules between molecularly smooth solid surfaces

Determination and prediction of critical coagulation concentrations

The transition between stability and coagulation, although in principle a gradual one, usually occurs over a reasonably small range of electrolyte concentration, and critical coagulation concentrations can be determined quite sharply. The exact value" of the critical coagulation concentration depends upon the criterion which is set for judging whether, or not, the sol is coagulated, and this must remain consistent during a series of investigations.

A common method for measuring critical coagulation concentrations is to prepare a series of about six small test tubes containing equal portions of the sol and to add to each, with stirring, the same volume of electrolyte in concentrations, allowing for dilution, which span the likely coagulation concentration. After standing for a few minutes, an approximate coagulation concentration is noted and a new set of sols is made up with a narrower range of electrolyte concentrations. After standing for a given time (e.g. 2 h), the sols are reagitated (to break the weaker interparticle bonds and bring small particles into contact with larger ones, thus

increasing the sharpness between stability and coagulation), left for a further period (e.g. 30 min) and then inspected for signs of coagulation. The critical coagulation concentration can be defined as the minimum electrolyte concentration which is required to produce a visible change in the sol appearance.

An expression for the critical coagulation concentration (c.c.c.) of an indifferent electrolyte can be derived by assuming that a potential energy curve such as *V (2)* in Figure 8.2 can be taken to represent the transition between stability and coagulation into the primary minimum. For such a curve, the conditions $V = 0$ and dV/d H = 0 hold for the same value of *H*. If V_R and V_A are expressed as in equations (7) and (10), respectively,

$$V = V_R + V_A = \frac{32\pi\varepsilon a k^2 T^2 \gamma^2}{e^2 z^2} \exp[-\kappa H] - \frac{Aa}{12H} = 0 \qquad \text{and}$$

$\frac{dV}{dH} = \frac{dV_R}{dH} + \frac{dV_A}{dH} = -\kappa V_R - \frac{V_A}{H} = 0$ from which $\kappa H = 1$; therefore,

$$\frac{32\pi\varepsilon a k^2 T^2 \gamma^2}{e^2 z^2} \exp[-1] - \frac{Aa\kappa}{12H} = 0 \qquad \text{gaining}$$

$\kappa_{coagulation} = \frac{443.8\varepsilon k^2 T^2 \gamma^2}{A e^2 z^2}$, substituting $\left(\frac{2e^2 N_A c z^2}{\varepsilon k T}\right)^{1/2}$ *for* κ *then*

$$c.c.c. = \frac{9.85x10^4 \varepsilon^3 k^5 T^5 \gamma^4}{N^A e^6 A^2 z^6} \qquad (14)$$

For an aqueous dispersion at 25°C, equation (14) becomes

$$c.c.c. = \frac{3.84x10^{-39} \gamma^4}{(A/J)^2 z^6} \qquad (15)$$

A number of features of the Deryagin-Landau-Verwey-Overbeek (D.L.V.O.) theory emerge from these expressions:

1. since y limits to unity at high potentials and to $ze\psi_d / 4kT$ at low potentials, critical coagulation concentrations are predicted to be proportional to $1/z^6$ at high potentials and to ψ_d^4 / z^2 at low potentials (see Figure 8.6). For a typical hydrosol, ψ_d will have an intermediate value in this respect, Taking 75 mV as a typical value for ψ_d (Figure 7.4), critical coagulation concentrations of inert electrolytes with z = 1, 2 and 3 are, for a given sol, predicted to be in the ratio 100 : 6.7 : 0.8. This is broadly in accord with experimental c.c.c. values, such as those presented in Table 8.1. The experimental values, however, tend to show a significantly stronger dependence on z than predicted above, and this probably reflects increased specific adsorption of counter-ions in the Stern layer with increasing z.
2. For a typical experimental hydrosol critical coagulation concentration at 25°C of 0.1 mol dm^{-3} for z = 1, and, again, taking ψ_d = 75 mV, the effective Hamaker constant, *A*, is calculated to be equal to 8 x 10^{-20} J. This is consistent with the order of magnitude of *A* which is predicted from the theory of London-van der Waals forces (see Table 8.3).
3. Critical coagulation concentrations for spherical particles of a given material should be proportional to e3 and independent of particle size. The definitions of the term 'critical coagulation concentration' *(a)* in relation to experimental measurements and *(b)* as a means for arriving at equation (8.14) are both arbitrary and, no doubt, slightly different from each other. In view of this (in addition to inevitable complications arising from specific ion adsorption and solvation), the results of critical coagulation concentration measurements can only be taken as support for the validity of the D.L.V.O. theory in its broadest outline. To make more detailed tests of stability theories, study of the kinetics of coagulation presents a better line of approach.

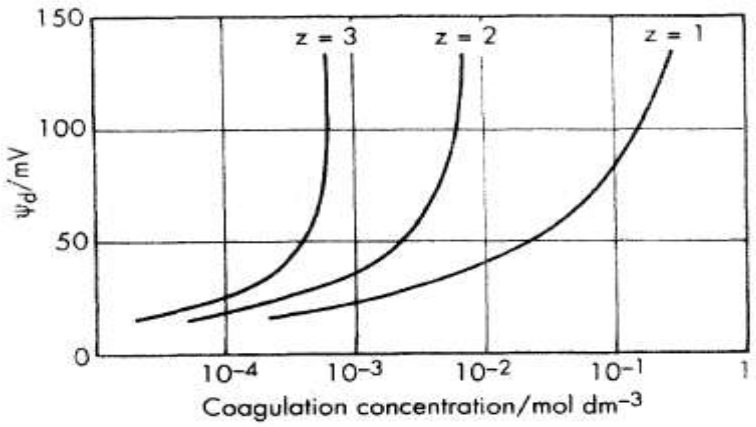

Figure 8.6 Coagulation concentrations calculated from equation (15), taking A – 10^{-19} J, for counter-ion charge numbers 1, 2 and 3. The sol is predicted to be stable above and to the left of each curve and coagulated below and to the right

Determination and prediction of critical coagulation concentrations

The transition between stability and coagulation, although in principle a gradual one, usually occurs over a reasonably small range of electrolyte concentration, and critical coagulation concentrations can be determined quite sharply. The exact value" of the critical coagulation concentration depends upon the criterion which is set for judging whether, or not, the sol is coagulated, and this must remain consistent during a series of investigations.

A common method for measuring critical coagulation concentrations is to prepare a series of about six small test tubes containing equal portions of the sol and to add to each, with stirring, the same volume of electrolyte in concentrations, allowing for dilution, which span the likely coagulation concentration. After standing for a few minutes, an approximate coagulation concentration is noted and a new set of sols is made up with a narrower range of electrolyte concentrations. After standing for a given time (e.g. 2 h), the sols are reagitated (to break the weaker interparticle bonds and bring small particles into contact with larger ones, thus increasing the sharpness between stability and coagulation), left for a

further period (e.g. 30 min) and then inspected for signs of coagulation. The critical coagulation concentration can be defined as the minimum electrolyte concentration which is required to produce a visible change in the sol appearance.

An expression for the critical coagulation concentration (c.c.c.) of an indifferent electrolyte can be derived by assuming that a potential energy curve such as *V (2)* in Figure 8.2 can be taken to represent the transition between stability and coagulation into the primary minimum. For such a curve, the conditions $V = 0$ and dV/d H = 0 hold for the same value of *H*. If V_R and V_A are expressed as in equations (7) and (10), respectively,

$$V = V_R + V_A = \frac{32\pi\varepsilon a k^2 T^2 \gamma^2}{e^2 z^2} \exp[-\kappa H] - \frac{Aa}{12H} = 0 \qquad \text{and}$$

$\frac{dV}{dH} = \frac{dV_R}{dH} + \frac{dV_A}{dH} = -\kappa V_R - \frac{V_A}{H} = 0$ from which $\kappa H = 1$; therefore,

$$\frac{32\pi\varepsilon a k^2 T^2 \gamma^2}{e^2 z^2} \exp[-1] - \frac{Aa\kappa}{12H} = 0 \qquad \text{gaining}$$

$\kappa_{coagulation} = \frac{443.8\varepsilon k^2 T^2 \gamma^2}{Ae^2 z^2}$, substituting $\left(\frac{2e^2 N_A c z^2}{\varepsilon k T}\right)^{1/2}$ *for* κ *then*

$$c.c.c. = \frac{9.85x10^4 \varepsilon^3 k^5 T^5 \gamma^4}{N^A e^6 A^2 z^6} \qquad (14)$$

For an aqueous dispersion at 25°C, equation (14) becomes

$$c.c.c. = \frac{3.84x10^{-39} \gamma^4}{(A/J)^2 z^6} \qquad (15)$$

A number of features of the Deryagin-Landau-Verwey-Overbeek (D.L.V.O.) theory emerge from these expressions:

1. since y limits to unity at high potentials and to $ze\psi_d / 4kT$ at low potentials, critical coagulation concentrations are predicted to be

proportional to $1/z^6$ at high potentials and to ψ_d^4 / z^2 at low potentials (see Figure 8.6). For a typical hydrosol, ψ_d will have an intermediate value in this respect, Taking 75 mV as a typical value for ψ_d (Figure 7.4), critical coagulation concentrations of inert electrolytes with z = 1, 2 and 3 are, for a given sol, predicted to be in the ratio 100 : 6.7 : 0.8. This is broadly in accord with experimental c.c.c. values, such as those presented in Table 8.1. The experimental values, however, tend to show a significantly stronger dependence on z than predicted above, and this probably reflects increased specific adsorption of counter-ions in the Stern layer with increasing z.

2. For a typical experimental hydrosol critical coagulation concentration at 25°C of 0.1 mol dm^{-3} for z = 1, and, again, taking ψ_d = 75 mV, the effective Hamaker constant, *A,* is calculated to be equal to 8 x 10^{-20} J. This is consistent with the order of magnitude of *A* which is predicted from the theory of London-van der Waals forces (see Table 8.3).
3. Critical coagulation concentrations for spherical particles of a given material should be proportional to e3 and independent of particle size. The definitions of the term 'critical coagulation concentration' *(a)* in relation to experimental measurements and *(b)* as a means for arriving at equation (8.14) are both arbitrary and, no doubt, slightly different from each other. In view of this (in addition to inevitable complications arising from specific ion adsorption and solvation), the results of critical coagulation concentration measurements can only be taken as support for the validity of the D.L.V.O. theory in its broadest outline. To make more detailed tests of stability theories, study of the kinetics of coagulation presents a better line of approach.

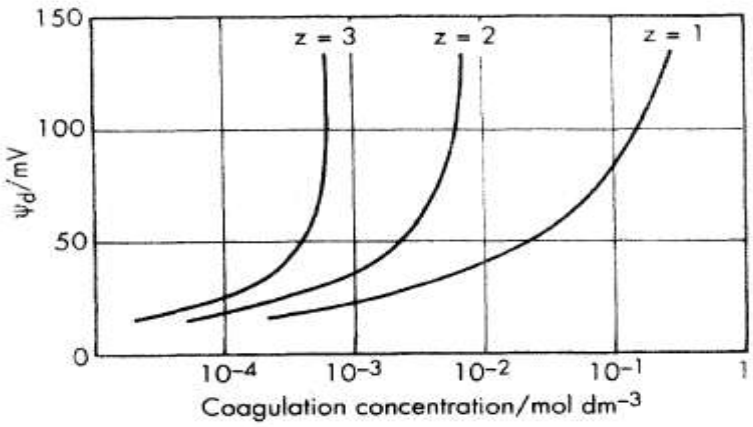

Figure 8.6 Coagulation concentrations calculated from equation (15), taking A – 10^{-19} J, for counter-ion charge numbers 1, 2 and 3. The sol is predicted to be stable above and to the left of each curve and coagulated below and to the right